Shahid Beheshti University

Pioneering Advances in Materials

Journal homepage: http://piadm.sbu.ac.ir ISSN: 3115-7114

Research paper

Investigation of Nonlinear Optical Properties of MoS_2 and MoO_x (x = 2, 3) Composite Thin Films

Fatemehsadat Hoseinizadeh[1], Javid Zamiranvari[1], Seyed Majid Mohseni[2], Rouhollah Karimzadeh[2]*

[1]*Department of Physics, Faculty of Science, Shahid Rajaee Teacher Training University, Lavizan, Tehran, Iran*
[2]*Department of Physics, Shahid Beheshti University, Tehran, Iran*

*r_karimzadeh@sbu.ac.ir

Article info:

Article history:

Received: 23/06/2026

Accepted: 20/07/2026

Keywords:

Transition Metal Dichalcogenides (TMDCs), Nonlinear Optical Properties, Saturable Absorption, Z-scan Technique, MoS_2–MoO_2–MoO_3 Composite Thin Films

Abstract

Recently, transition metal dichalcogenide (TMDC) materials have attracted considerable attention due to their excellent nonlinear optical (NLO) properties. Their unique characteristics, including ultra-broadband absorption, strong nonlinear optical responses, and potential applications in optical limiting, saturable absorption, pulsed laser generation, and biosensing, have been extensively studied. In this work, we report, for the first time, an investigation of the nonlinear optical properties of FTO/MoS_2–MoO_2–MoO_3 composite thin films deposited on fluorine-doped tin oxide (FTO) substrates by electrodeposition. Strong light–matter interactions under high-intensity laser irradiation can induce nonlinear optical responses in such materials. Therefore, the nonlinear absorption and nonlinear refraction characteristics of the prepared films were examined using the Z-scan technique under continuous-wave laser excitation at 532 nm with an output power of 180 mW. The obtained results reveal pronounced saturable absorption behavior. The observations indicate that nonlinear absorption and nonlinear refraction are negligible at low laser powers; however, at higher laser intensities, significant nonlinear optical effects emerge. Furthermore, modifications in the chemical composition of the material, specifically a decrease in sulfur content accompanied by an increase in oxygen content, lead to enhanced nonlinear absorption and reduced nonlinear refraction. These findings demonstrate the strong dependence of the nonlinear optical response on both the excitation intensity and the chemical structure of the MoS_2–MoO_2–MoO_3 composite films.

1. Introduction

Two-dimensional (2D) materials have attracted significant attention in recent years due to their remarkable physical, chemical, and optical properties, which have enabled numerous applications in science and industry [1-3]. Among these properties, nonlinear optical (NLO) responses are of particular interest because of their potential use in photonic and optoelectronic devices. Owing to their atomically thin structures, strong light–matter interactions, and tunable electronic properties, 2D materials exhibit enhanced optical nonlinearities that can be exploited in applications such as mode-locking, optical switching, optical modulation, and ultrafast laser systems.

Since the discovery of graphene, which pioneered the field of 2D materials, a wide range of layered nanomaterials have been investigated for nonlinear photonic applications [4]. These include topological insulators [4-7], black phosphorus [8], MXenes [9, 10], graphitic carbon nitride [11], metal–organic hybrid materials [12], and transition metal dichalcogenides (TMDCs) [13-15]. The rapid development of these materials has opened new opportunities in physics, chemistry, biology, energy technologies, and photonics [1-3]. Since around 2009, nonlinear photonics based on 2D materials has emerged as an important research area due to the unique optical characteristics of these materials [16-19]. The attractiveness of 2D materials for nonlinear optics arises from several key features, including large and ultrafast nonlinear optical responses, broadband and tunable optical absorption, short carrier recovery times, high optical damage thresholds, excellent thermal and chemical stability, and relatively low fabrication costs. These advantages make them promising candidates for next-generation photonic devices. Nonlinear optics describes the interaction of intense light with matter, where the optical response of a material becomes dependent on the intensity of the incident electric field. Such effects typically occur when the electric field of the incident laser approaches the strength of interatomic fields [20]. Under these conditions, materials may exhibit nonlinear absorption, nonlinear refraction, harmonic generation, and other higher-order optical phenomena.

Among 2D materials, TMDCs have attracted particular interest because of their strong nonlinear optical responses. Atomically thin TMDCs exhibit efficient second- and third-harmonic generation. Monolayer TMDCs, which lack inversion symmetry, possess exceptionally large second-order nonlinear susceptibilities, significantly exceeding those of many conventional dielectric materials [17, 18]. In contrast, even-layered structures with inversion symmetry primarily exhibit third-order nonlinear optical effects [19, 21 ,22]. Studies have demonstrated strong second-harmonic generation in monolayer MoS_2 excited by near-infrared laser radiation, with the nonlinear response strongly influenced by the number of layers, excitation wavelength, and structural quality of the material [23-26].

Various experimental techniques have been employed to characterize the nonlinear optical properties of these materials, among which the Z-scan method is one of the most widely used [27]. This technique provides simultaneous measurements of nonlinear absorption and nonlinear refraction, making it a powerful tool for evaluating optical nonlinearities [28].

A major breakthrough in the field occurred in 2013 when saturable absorption was reported in multilayer MoS_2.

Ultrafast saturable absorption was observed in liquid-phase-exfoliated MoS_2 nanosheets under femtosecond laser excitation, with performance surpassing that of graphene under similar conditions [29-33]. Subsequently, broadband saturable absorption was demonstrated and successfully applied in mode-locked fiber lasers, highlighting the potential of TMDCs as optical modulators and pulse-generation materials [29]. In addition to saturable absorption, MoS_2 exhibits optical limiting behavior, where optical transmission decreases with increasing incident intensity, providing protection against high-power laser radiation [34]. The nonlinear optical response of TMDCs is strongly dependent on factors such as layer number, excitation wavelength, chemical composition, and defect density [35]. Furthermore, transitions between saturable absorption and optical limiting behavior have been observed under different excitation conditions [36, 37]. Under near-infrared excitation, two-photon absorption may become the dominant nonlinear process due to the relationship between the excitation energy and the material bandgap [38]. Besides MoS_2, molybdenum oxides such as MoO_2 and MoO_3 have attracted interest because of their unique electrical and optical properties. MoO_2 exhibits metallic-like conductivity and semimetallic behavior [25-27], whereas MoO_3 is an n-type semiconductor with a wide bandgap resulting from oxygen vacancies. The integration of TMDCs and molybdenum oxides offers promising opportunities for tailoring nonlinear optical responses and developing advanced photonic materials. Overall, 2D materials have become key components in modern nonlinear photonics and are being widely explored for applications in fiber lasers, solid-state lasers, waveguide lasers, optical limiters, optical switches, optical modulators, optical polarizers, and all-optical devices. In this work, FTO/MoS_2–MoO_2–MoO_3 composite thin films were fabricated by electrodeposition, and their linear and nonlinear optical properties were systematically investigated. The nonlinear absorption and nonlinear refraction characteristics were evaluated using the open- and closed-aperture Z-scan techniques under continuous-wave laser excitation at 532 nm. The influence of film composition, particularly the sulfur-to-oxygen ratio, on the optical response of the films was also examined.

2. Materials and method

In this study, the electrodeposition method was used for prepare the samples. Using this method, high-quality structures with low cost can be produced by controlling the amount of composite materials. 3 samples FTO/MoS_2, MoO_2, MoO_3 where sample A was deposited with current density of 4 mA/cm^2 for 12.5 seconds, sample B was deposited with current density of 8 mA/cm^2 for 6.25 second and sample C was deposited with current density of 20 mA/cm^2 for 2.5 seconds by electrodeposition method [39]. Due to the control of the deposition time and current, the thickness of the deposited material in all samples is 8.3 nm. UV-Vis absorption spectra were prepared to investigate changes in the chemical structure of the samples. The linear absorption coefficient of the samples was investigated using the transfer technique. The nonlinear optical properties of the samples have been studied using the z-scan method. The nonlinear absorption coefficient was measured using the open aperture z-scan method and the nonlinear refractive index was measured using the closed aperture z-scan method. In this method, a Gaussian laser beam is focused to a narrow range and the sample moves along the z-direction. In this study, a continuous wave laser with a wavelength of 532 nm was used as the wave emission source. The 180mw laser beam is focused using a converging lens with a focal length of 50 cm. The laser beam radius at the focus is about 0.13mm. The power of the transmitted light is measured by a detector.

3. Results and discussion

UV–Vis absorption spectra were acquired in the wavelength range of 300–1000 nm, as presented in Figure 1. Multiple absorption features corresponding to intraband and interband transitions are observed. The low-energy absorption bands, which are typically attributed to the A and B excitonic transitions of MoS_2, do not coincide exactly with the reported wavelengths of 623 and 683 nm [40]. In addition, the excitonic features are not well separated and appear considerably broadened, indicating possible structural disorder, compositional variations, or interactions with oxide phases in the films.

Based on the findings reported in Ref [41], the coexistence of MoO_2 and MoS_2 phases may account for the absence of the characteristic MoS_2 excitonic peaks at approximately 623 and 683 nm in the UV–Vis spectra. The electronic interaction between these phases is likely to modify the valence-band structure of MoS_2, causing the excitonic transitions to broaden or diminish. While MoO_3 is also present in the films, its contribution to excitonic behavior is expected to be negligible. The obtained spectra therefore reflect the combined optical characteristics of both MoS_2 and MoO_x phases. In addition, an increase in deposition current results in reduced sulfur incorporation and increased oxygen content, which is accompanied by a corresponding increase in optical absorption.

The transmission technique was used to investigate the optical properties of the samples and linear absorption coefficients. Figure 2 shows a transmission measurement of samples A, B, and C (output power versus input power) under continuous wave laser irradiation with a wavelength of 532 nm.

The solid dots are the measured experimental data and the bold lines in this figure are obtained from samples A, B, C based on the linear absorption theory.

The measured linear absorption coefficients of these samples are large numbers, as listed in Table 1. In the graph in Figure 2, it can be seen that reducing the amount of sulfur and increasing the amount of oxygen in the chemical composition of the samples is effective in increasing the linear absorption rate.

The z-scan method was used to investigate the nonlinear optical properties of the samples. The nonlinear absorption coefficients of the samples were measured with the open aperture z-scan method under the same conditions for all samples. In this experiment, a 180 mW continuous-wave laser beam at a wavelength of 532 nm was directed onto the samples using a lens with a focal length of 50 cm.

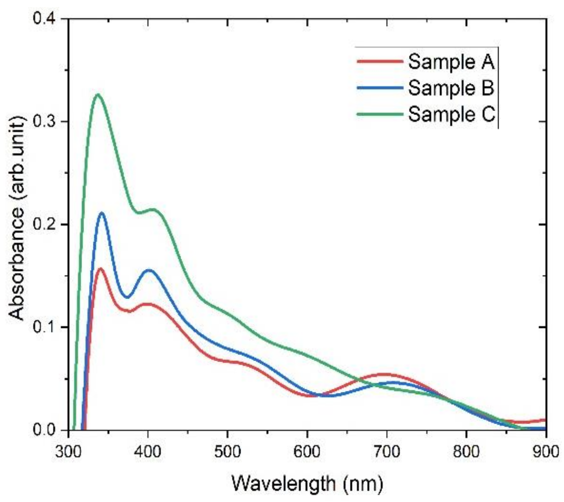

Figure 1. UV-Vis absorption spectra of samples A, B, and C with red, blue, and green plots, respectively

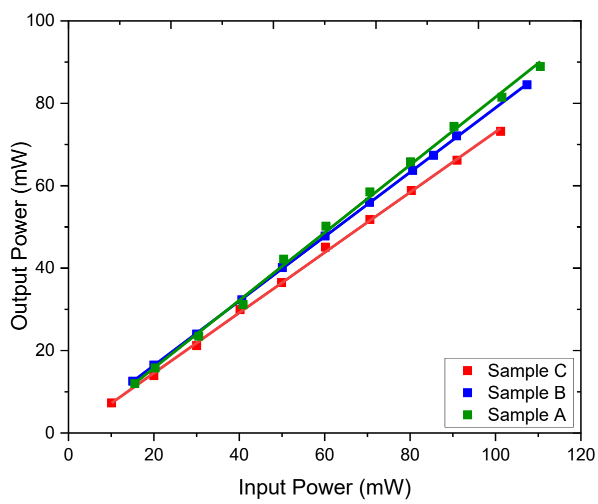

Figure 2. Linear absorption of samples A, B, C using a 532nm laser. The green, blue, and red dots are the measured experimental data and the green, blue, and red lines are the fitted plots of samples A, B, and C, respectively

The samples were translated along the optical axis (from −z to +z), and the transmitted power was measured as a function of sample position using a detector.
The obtained data were fitted using Eq. (1), and the corresponding Z-scan curves were plotted accordingly.

$$T = \frac{1}{\beta I_0 L_{eff}} \quad (1)$$

$$(1 + (z/z_0)^2)\ln(1 + \frac{\beta I_0 L_{eff}}{1 + (z/z_0)^2})$$

Plotted in terms of normalized transmission versus sample location (Figure 3). Z is the distance of the samples from the focal point of the lens, Z_0 is the Rayleigh length before the lens. According to the Z-scan results, the absorption is linear at the beginning and end of the scan. However, as the sample approaches the focal point of the lens and the light intensity increases, nonlinear optical effects become significant. The symmetric nature of the transmittance curves around the focal position indicates the presence of saturable absorption in the samples. The observed behavior suggests that increasing current density and decreasing deposition time, which correspond to a decrease in sulfur content and an increase in oxygen content, enhances the saturable absorption response. The nonlinear absorption coefficient (β) was calculated, and the obtained values are reported in Table 1. The closed-aperture Z-scan technique was employed to measure the nonlinear refractive index of the samples. In this experimental setup, a continuous-wave laser operating at 532 nm and a lens with a focal length of 500 mm were used to focus the laser beam. The samples were translated along the optical axis from −z to +z, and the transmitted power passing through both the sample and the aperture was recorded by a detector as a function of sample position.
As the nonlinear material approaches the focal region, the intensity of the incident laser beam increases, giving rise to nonlinear optical effects. Under these conditions, both nonlinear absorption and nonlinear refraction influence the beam reaching the detector.
Near the focal point, the reduction in the beam cross-sectional area results in increased irradiance, leading to a self-lensing effect within the sample. For a positive nonlinear refractive index, the sample behaves as an additional converging lens, causing the focal point to shift toward the focusing lens.
As a consequence of this focal shift, the beam divergence at the aperture initially increases, reducing the amount of light transmitted through the aperture and producing a valley in the transmittance-versus-position curve. After the sample passes through the focal region, the self-lensing effect causes the beam to become more convergent at the aperture plane, increasing the transmitted intensity and generating a peak in the transmittance curve.
The characteristic valley–peak configuration indicates positive nonlinear refraction (self-focusing).
To isolate the nonlinear refractive contribution, the effect of nonlinear absorption was removed by dividing the closed-aperture Z-scan data by the corresponding open-aperture Z-scan data.

Table 1. Linear absorption, nonlinear absorption, and nonlinear refraction coefficients obtained from samples A, B, and C under 532 nm continuous wave laser irradiation

sample	Linear absorption coefficient (cm^{-1})	Nonlinear absorption coefficient(cm/w)	Nonlinear refracthion coefficient(cm^2/w)
A	2.36×10^5	$(-1.11 \pm 0.007) \times 10^3$	0.72 ± 0.04
B	2.97×10^5	$(-1.23 \pm 0.007) \times 10^3$	0.38 ± 0.02
C	3.76×10^5	$(-1.33 \pm 0.01) \times 10^3$	0.36 ± 0.01

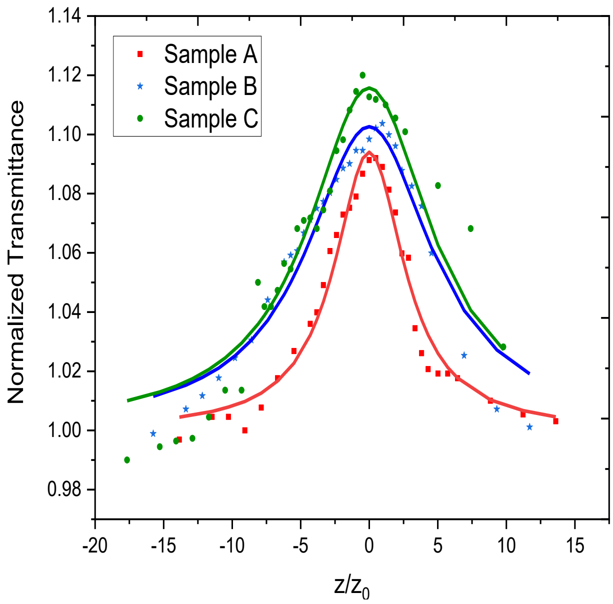

Figure 3. Data from open aperture Z-scan; nonlinear saturation absorption of samples A, B, C using a 532 nm laser. red, blue, and green dots are the measured experimental data and red, blue, and green lines are the fitted plots of samples A, B, and C, respectively

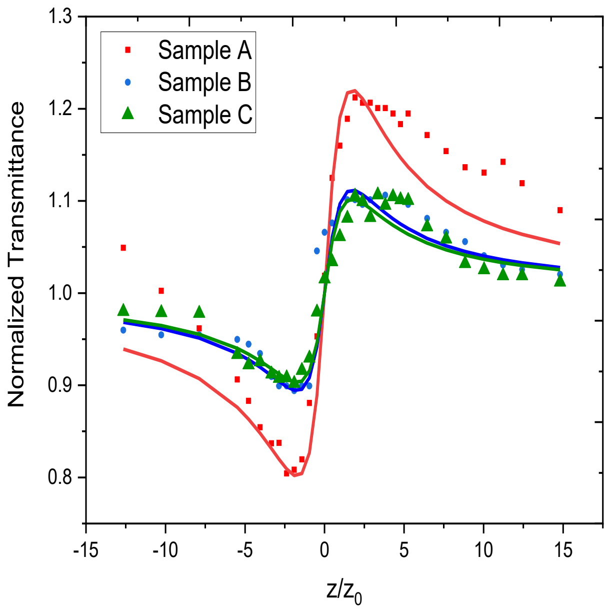

Figure 4. Data from open-aperture Z-scan; nonlinear saturation absorption of samples A, B, C using a 532nm laser. Red, blue, and green dots are the measured experimental data and red, blue, and green lines are the fitted plots of samples A, B, and C, respectively

The resulting experimental data were fitted using Eq. (2), which describes the thermal-lens-induced phase distortion based on the aberration model. The fitted results are presented in Figure 4 as normalized transmittance versus sample position. The transmittance data were normalized by dividing each measured value by the average of the transmittance values obtained at the beginning and end of the scan, where nonlinear effects are negligible.

$$T = \left(1 + \frac{\theta}{2}\, tan^{-1}\left(\frac{2(z/z_0)}{3 + (z/z_0)^2}\right)\right)^2 \qquad (2)$$

By fitting the experimental data to Eq. (2) and obtaining $\theta = kI_0L_{eff}n_2$, the nonlinear refractive index n_2 can be calculated. In all closed-aperture Z-scan curves, a valley is observed before a peak, indicating a self-focusing effect and, consequently, a positive nonlinear refractive index. The values of the nonlinear refractive index reported in Table 1 confirm this observation, as all measured values are positive. Furthermore, the Z-scan curves show that the separation between the valley and peak decreases with increasing deposition current. Since higher deposition currents result in a lower sulfur content and a higher oxygen content in the films, the nonlinear refractive index is found to decrease as the oxygen concentration increases.

4. Conclusion

In this study, the nonlinear absorption and nonlinear refraction coefficients of FTO/MoS_2–MoO_2–MoO_3 composite thin films were investigated using the open- and closed-aperture Z-scan techniques under continuous-wave laser excitation at 532 nm with an output power of 180 mW. In addition, the linear absorption coefficients of the samples were measured. The experimental results indicate that both laser intensity and material composition play important roles in determining the nonlinear optical response. The samples exhibited negligible nonlinear effects at low laser powers; therefore, the highest available laser power was employed for the measurements. Furthermore, variations in the deposition conditions significantly affected the film composition. Increasing the deposition current density while reducing the deposition time led to a decrease in sulfur content and an increase in oxygen content within the films. The optical characterization results revealed that changes in the sulfur-to-oxygen ratio strongly influence the optical properties of the composites. Specifically, an increase in oxygen content was associated with enhanced linear absorption, stronger saturable absorption behavior, and a reduction in the nonlinear refractive index. These findings demonstrate that the nonlinear optical properties of MoS_2–MoO_2–MoO_3 composite films can be effectively tailored through compositional control. The observed optical characteristics make these materials promising candidates for applications involving high-power lasers, ultrashort optical pulses, and high-intensity light propagation. Potential applications include pulsed and high-power laser systems, laser amplifiers, fiber-optic and optical communication technologies, industrial and medical laser devices, nonlinear photonic components, quantum information processing, and optical windows and sensors for aerospace and defense applications.

References

[1] A.S, Shalahuddin. Pengemb Apl Berbas android yang menampilkan Mater belajar disertai animasi peraga terkait Mater yang disajikan serta Latih soal yang dapat langsung dikerjakan oleh pengguna. 2018;1(1):1.

[2] Kong X, Liu Q, Zhang C, Peng Z, Chen Q. Elemental two-dimensional nanosheets beyond graphene. Chem Soc Rev [Internet]. 2017;46(8):2127-57. Available from: https://doi.org/10.1039/C6CS00937A

[3] Bhimanapati GR, Lin Z, Meunier V, Jung Y, Cha J, Das S, et al. Recent advances in two-dimensional materials beyond graphene. ACS Nano. 2015;9(12):11509-39.

[4] Wu J, Lin H, Moss DJ, Loh KP, Jia B. Graphene oxide for photonics, electronics and optoelectronics. 2023;(Graphene oxide for photonics, electronics and optoelectronics):22.

[5] Hua Z. Review-ultrathin two-dimensional nanomaterials. ACS Nano. 2015;(Xx).

[6] Tan C, Cao X, Wu XJ, He Q, Yang J, Zhang X, et al. Recent advances in ultrathin two-dimensional nanomaterials. Chem Rev. 2017;117(9):6225-331.

[7] Kinloch IA, Suhr J, Lou J, Young RJ, Ajayan PM. Composites with carbon nanotubes and graphene: an outlook. Science. 2018;362(6414):547-53.

[8] Wang QH, Kalantar-Zadeh K, Kis A, Coleman JN, Strano MS. Q. H. Wang, K. Kalantarzadeh, A. Kis, J. N. Coleman, M. S. Strano, Nat. Nanotechnol. 2012, 7, 699. Nat Nanotechnol [Internet]. 2012;7(11):699-712. Available from: https://doi.org/10.1038/nnano.2012.193

[9] Dhanabalan SC, Ponraj JS, Guo Z, Li S, Bao Q, Zhang H. Emerging trends in phosphorene fabrication towards next generation devices. Adv Sci. 2017;4(6).

[10] Luo M, Fan T, Zhou Y, Zhang H, Mei L. 2D black phosphorus-based biomedical applications. Adv Funct Mater. 2019;29(13):1-19.

[11] Molle A, Goldberger J, Houssa M, Xu Y, Zhang SC, Akinwande D. Buckled two-dimensional Xene sheets. Nat Mater. 2017;16(2):163-9.

[12] Low T, Chaves A, Caldwell JD, Kumar A, Fang NX, Avouris P, et al. Polaritons in layered two-dimensional materials. Nat Mater. 2017;16(2):182-94.

[13] Song CL, Wang YL, Jiang YP, Zhang Y, Chang CZ, Wang L, et al. Topological insulator Bi2 Se3 thin films grown on double-layer graphene by molecular beam epitaxy. Appl Phys Lett.

2010;97(14).

[14] Moore JE. The birth of topological insulators. Nature. 2010;464(7286):194-8.

[15] Zhao C, Zhang H, Qi X, Chen Y, Wang Z, Wen S, et al. Ultra-short pulse generation by a topological insulator based saturable absorber. Appl Phys Lett. 2012;101(21).

[16] Boyd RW, Shi Z, De Leon I. The third-order nonlinear optical susceptibility of gold. Opt Commun [Internet]. 2014;326:74-9. Available from: https://doi.org/10.1016/j.optcom.2014.03.005

[17] Zhou X, Cheng J, Zhou Y, Cao T, Hong H, Liao Z, et al. Strong second-harmonic generation in atomic layered GaSe. J Am Chem Soc. 2015;137(25):7994-7.

[18] Crespi V, Liu Z. Extraordinary second harmonic generation in tungsten disulfide monolayers. 1(c):1-5.

[19] Woodward RI, Murray RT, Phelan CF, De Oliveira REP, Runcorn TH, Kelleher EJR, et al. Characterization of the second- and third-order nonlinear optical susceptibilities of monolayer MoS2 using multiphoton microscopy. 2D Mater. 2017;4(1).

[20] Jost B, Sergienko A, Abouraddy A, Saleh B, Teich M. Spatial correlations of spontaneously down-converted photon pairs detected with a single-photon-sensitive CCD camera. Opt Express. 1998;3(2):81.

[21] Wang R, Chien HC, Kumar J, Kumar N, Chiu HY, Zhao H. Third-harmonic generation in ultrathin films of MoS2. ACS Appl Mater Interfaces. 2014;6(1):314-8.

[22] Wu R, Zhang Y, Yan S, Bian F, Wang W, Bai X, et al. Purely coherent nonlinear optical response in solution dispersions of graphene sheets. Nano Lett. 2011;11(12):5159-64.

[23] Kumar N, Najmaei S, Cui Q, Ceballos F, Ajayan PM, Lou J, et al. Second harmonic microscopy of monolayer MoS2. Phys Rev B Condens Matter Mater Phys. 2013;87(16):25-7.

[24] Malard LM, Alencar TV, Barboza APM, Mak KF, De Paula AM. Observation of intense second harmonic generation from MoS2 atomic crystals. Phys Rev B Condens Matter Mater Phys. 2013;87(20):1-5.

[25] Clark DJ, Senthilkumar V, Le CT, Weerawarne DL, Shim B, Jang JI, et al. Strong optical nonlinearity of CVD-grown MoS2 monolayer as probed by wavelength-dependent second-harmonic generation. Phys Rev B Condens Matter Mater Phys. 2014;90(12):1-5.

[26] Yin X, Ye Z, Chenet DA, Ye Y, O'Brien K, Hone JC, et al. Edge nonlinear optics on a MoS2 atomic monolayer. Science. 2014;344(6183):488-90.

[27] De Araújo CB, Gomes ASL, Boudebs G. Techniques for nonlinear optical characterization of materials: a review. Reports Prog Phys. 2016;79(3).

[28] Changaei S, Zamir-Anvari J, Heydari NS, Ghayeb Zamharir S, Arshadi M, Bahrami B, et al. The large and tunable nonlinear absorption response of graphene oxide liquid crystals.pdf.

[29] Wang K, Wang J, Fan J, Lotya M, O'Neill A, Fox D, et al. Ultrafast saturable absorption of related papers. ACS Nano. 2013;7.

[30] Xie Y, Zhang B, Wang S, Wang D, Wang A, Wang Z, et al. Ultrabroadband MoS2 photodetector with spectral response from 445 to 2717 nm. Adv Mater. 2017;29(17).

[31] Dhasmana N, Fadil D, Kaul AB, Thomas J. Investigation of nonlinear optical properties of exfoliated MoS2 using Photoacoustic Zscan. Soft Mater Biomater [Internet]. 2016;1. Available from: https://journals.cambridge.org/abstract_S2059852116005296

[32] Balaei M, Karimzadeh R, Naseri T. Introducing a novel approach to linear and nonlinear electrical

conductivity of MoS2.pdf. 2021.

[33] Rahmati B, Ghayeb S, Rouhollha Z, Seyed K, Mohseni M. Nonlinear optical properties of vertically-aligned MoS2 nanosheets. J Electron Mater [Internet]. 2021;(0123456789). Available from: https://doi.org/10.1007/s11664-021-08885-w

[34] Balaei M, Karimzadeh R, Saghaei H, G-Z S. The effect of laser wavelength and concentration on the optical limiting response of exfoliated MoS2 in the NMP solvent.pdf. 2021.

[35] Ouyang Q, Yu H, Zhang K, Chen Y. Saturable absorption and the changeover from saturable absorption to reverse saturable absorption of MoS2 nanoflake array films. J Mater Chem C. 2014;2(31):6319-25.

[36] Li Y, Dong N, Zhang S, Zhang X, Feng Y, Wang K, et al. Giant two-photon absorption in monolayer MoS2. Laser Photonics Rev. 2015;9(4):427-34.

[37] Zhao M, Chang MJ, Wang Q, Zhu ZT, Zhai XP, Zirak M, et al. Unexpected optical limiting properties from MoS2 nanosheets modified by a semiconductive polymer. Chem Commun [Internet]. 2015;51(61):12262-5. Available from: https://doi.org/10.1039/C5CC01819F

[38] Wang K, Feng Y, Chang C, Zhan J, Wang C, Zhao Q, et al. Broadband ultrafast nonlinear absorption and nonlinear refraction of layered molybdenum dichalcogenide semiconductors. Nanoscale. 2014;6(18):10530-5.

[39] Mokhtari S, M M, Arshadi Pirlar M, Karimzadeh R, J L. Sulfur reduction in MoSO composite towards fabrication of porous structures: physical and nonlinear optical effects.pdf. 2021.

[40] Visic B, Dominko R, Gunde MK, Hauptman N, Skapin SD, Remskar M. Optical properties of exfoliated MoS2 coaxial nanotubes: analogues of graphene. Nanoscale Res Lett. 2011;6:1-6.

[41] Erfanifam S, Mohseni SM, Jamilpanah L, Mohammadbeigi M, Sangpour P, Hosseini SA, et al. Tunable bandgap and spin-orbit coupling by composition control of MoS2 and MoOx (x = 2 and 3) thin film compounds. Mater Des [Internet]. 2017;122:220-5. Available from: https://doi.org/10.1016/j.matdes.2017.02.085